

## **Microscopic and macroscopic points of view of gas hydrate formation using *in-situ* Raman spectroscopy**

\*Ju Dong Lee, Sang Yeon Hong, SeungMin Lee

*Offshore Plant Resources R&D Center, Korea Institute of Industrial Technology  
julee@kitech.re.kr*

### **ABSTRACT**

In order to fully understand the influence of kinetic inhibitor, poly N-vinylcaprolactam (PVCap), on methane hydrate formation, gas uptake measurement and in-situ Raman spectroscopic analysis were carried out simultaneously in a semi-batch stirred tank reactor at constant temperature and pressure. The capturing behavior of guest molecules (large to small cavity ratio or cage variation) is one of the most important properties of gas hydrate studies. However the real-time properties of the cage variation under constant T & P conditions in an agitation system have not been reported previously. In this study we measured this property (i.e., the large to small cavity ratio) from the *in-situ* Raman spectra during hydrate formation in an agitation system instead of a static system, which provided valuable information on the time-dependent hydrate kinetic behavior. The study reveals that the presence of PVCap prevents the rate of large cavity encapsulation at an early stage of hydrate formation. The influence of PVCap from microscopic and macroscopic points of view is also presented.

### **1. INTRODUCTION**

Gas hydrates are non-stoichiometric ice-like solid compounds consisting of small gas molecules and water molecules[Kashchiev (2003)]. Generally, gas hydrates have three basic crystal structures where gas molecules are enclathrated in cavity structures that are formed by hydrogen-bonded water molecules[Kelland(2006), Zhang(2004)]. They have attracted attention because of their great potential to be used as a gas storage and capturing medium. However, natural gas hydrate formation can cause blockages in subsea gas and oil flow lines, which can lead to catastrophic economic loss and ecological risks[Kelland(2006), Koh(2002)]. Therefore, many researchers have tried to apply various inhibitors to delay the formation rate of gas hydrates because the prevention and removal of hydrates during natural gas and oil subsea production and transportation are major concerns to the energy industries [Sloan (1998), Mohammad (2010)]. There are three classes of hydrate inhibitors; thermodynamic, anti-agglomerant, and kinetic inhibitors. Kinetic hydrate inhibitors (KHIs) are a class of low dosage hydrate inhibitor (LDHI) and are commercial materials often used in the upstream oil and gas industry[Heidaryan(2010)]. They are usually water soluble polymers and are effective at concentrations typically ten to one hundred times less than ethylene glycol

or methanol concentrations[Dalton York(2008)]. KHI s are effective at concentrations as low as 0.5 wt%, however the optimum concentration of KHI s are varied depends on fields conditions between 0.5 and 3.0 wt%[Jinhai Yang(2011)]. It is generally suggested that the kinetic inhibitors hinder hydrate formation by adsorbing to the surface of hydrate crystals, and also by sterically blocking guest molecules from entering and completing a hydrate cavity[Kelland(2006), Makogon(2002)]. Adsorption of kinetic inhibitors to the surface of hydrate has been studied extensively by Makogon(2002) and Carver(1995) et al. They found that kinetic inhibitors with lactam pendant groups adsorb to the hydrate surface with the lactam ring sterically stabilized in the large cavity. However, there is still a significant knowledge gap to fully understand the inhibition mechanism of kinetic inhibitors[Jinhai Yang(2011), Makogon(2002)].

## 2. Apparatus and Results

In this study, the influence of a kinetic inhibitor, poly N-vinylcaprolactam (PVCap), on methane hydrate formation was investigated. In order to get vital information for cage occupancy and capturing kinetics of guest molecules, in-situ Raman analysis and gas uptake measurement (kinetic experiment) were carried out simultaneously. We present the molecular level of structure I (sI) hydrate cavity behaviors as well as traditional hydrate kinetic data, which have not been reported previously.

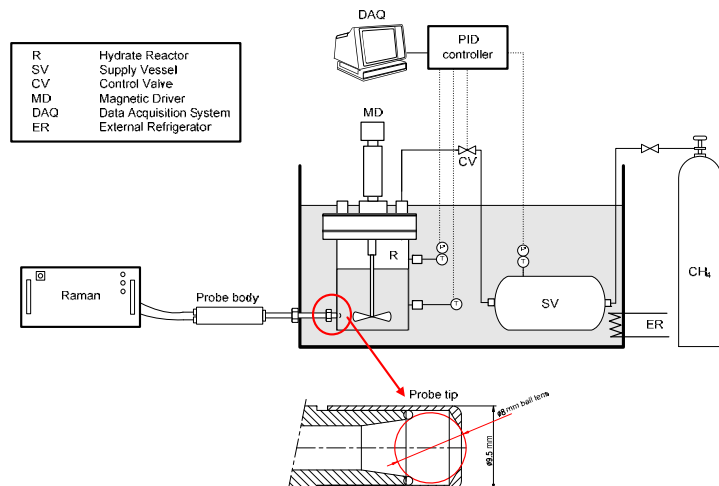


Fig. 1 Schematic diagram of experimental apparatus

The experimental apparatus, as shown Fig. 1, mainly consists of a stainless-steel reactor (372.5 ml), a supply vessel (566.5 ml), refrigeration system, water bath, data acquisition system and a real-time Raman spectroscopy. As described in Figure 1, we conducted in-situ Raman spectroscopic analysis during the experiments of hydrate formation. The probe tip with experimental setup was designed for use at high pressure and slurry or suspended particle system.

Table 1 gives a summary of experimental results for methane hydrate formation along with induction time, gas consumption ( $\Delta n$ ), water to hydrate conversion ( $x$ ) and large to small cavity ratio ( $L/S$ ). Each experimental run was conducted in the absence or the presence of PVCap (0.04 wt%) under constant temperature and pressure conditions.

The  $\Delta n$ ,  $x$  and  $L/S$  were measured after 700 min after the beginning of experiment, and the results are listed in Table 1. The hydrate conversion was calculated by assuming that the cage occupancy of  $\text{CH}_4$  is 100% in both the small and large cages. In this paper 5.75 was referred to as hydration number.

System	#	induction time (min)	gas consumption after 700min, $\Delta n$ (mol)	Water to hydrate conversion after 700min, $x$ (%)	Large to small cavity ratio after 700min, $L/S$
Pure water	1	5	1.006	77.1	3.29
	2	6	1.002	76.8	2.95
	3	4	0.998	76.5	3.13
0.04 wt % PVCap	4	174	0.671	51.4	2.90
	5	134	0.664	50.9	2.88
	6	153	0.654	50.1	2.85

Table. 1 Summary of experimental results for methane hydrate formation with or without PVCap at 274.15K and 5.0 MPa

All experiments showed similar patterns on the gas uptake measurement, and therefore only two experimental runs (experiments #1 and #4 as listed in Table 1 and Figure 2) were selected for further Raman analysis. Figure 2 shows the formation rate of  $\text{CH}_4$  gas hydrate with pure water and 0.04 wt% PVCap at 274.15 K and 5.0 MPa. (subcooling = 5.7K). The formation rate of  $\text{CH}_4$  hydrate with PVCap was significantly less than that of the pure water system. The hydrate nucleation was also significantly delayed in the presence of PVCap. The induction time of the system with PVCap was 174 min, whereas that of the pure water system was 5 min at given experimental conditions.

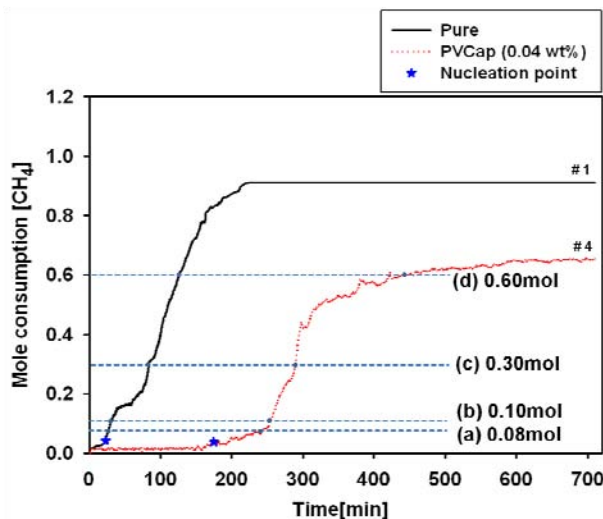


Fig. 2 Comparison of kinetics of  $\text{CH}_4$  hydrate formation with pure water and 0.04 wt% PVCap

In the early stage of hydrate formation after the nucleation point, the system with PVCap showed very slow hydrate formation. Subsequently, 250 min after the beginning

of experiment, the rate of gas consumption was increased, which is shown in Figure 2. As presented in the Figure 3, the gas uptake measurement and the Raman intensity data shows quite similar trend as function of time. In addition the first appearance of Raman signals (at 2905 and  $2915\text{ cm}^{-1}$ ) indicates exact induction time which was monitored from gas uptake measurement. Therefore it was concluded that the Raman spectra obtained from the moving hydrate particles in a stirred tank reactor can be used to describe the state of kinetic behavior.

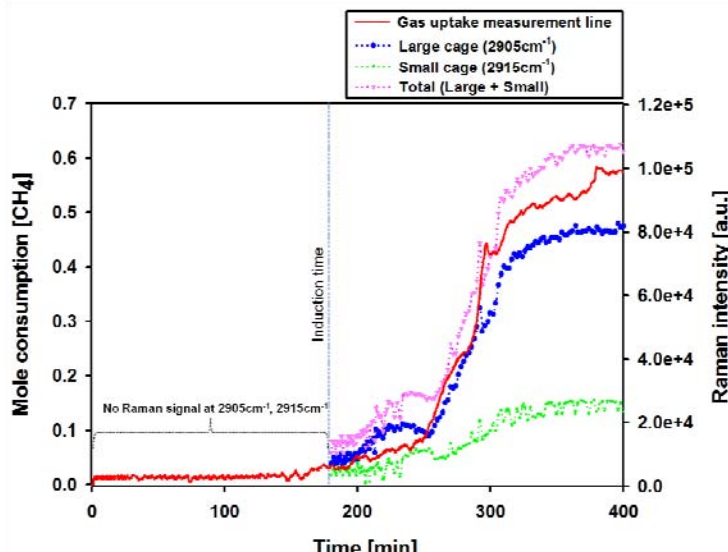


Fig. 3 Comparison of kinetics & Raman peak intensity of  $\text{CH}_4$  hydrate formation with 0.04 wt% PVCap

In all experiments, sufficient experimental time was given in order to perform full conversion of hydrate formation. Theoretically, 1.3 moles of  $\text{CH}_4$  should be required for the full conversion of hydrate formation at the given water amount (135 ml). As shown in Figure 2, the system with pure water reached around 77% of the theoretical value of conversion. However the system with 0.04 wt% PVCap showed a maximum of 51% hydrate conversion even though sufficient time (700 min) was given. This indicates that the PVCap significantly delays hydrate nucleation and also prevents further gas hydrate growth.

As shown in Figure 2, when the amount of gas consumption reached specific levels (0.08, 0.1, 0.3 and 0.6 mole consumption), each in-situ Raman spectrum was obtained, which are plotted in Figure 4. The large to small cavity ratios, determined by Raman spectra, are also shown in Figure 4. The Raman bands at  $2905\text{ cm}^{-1}$  and  $2915\text{ cm}^{-1}$  stand for the C-H stretching mode from  $\text{CH}_4$  encapsulated in large and small cages respectively. It is also known that structure I (sl) has two different cages that consist of 6 large cavities ( $5^{12}6^2$ ) and 2 small cavities ( $5^{12}$ ) per unit cell. Hence, the ratio of large to small cavities theoretically should be 3[Sloan(2003)].

When the system reached 0.08 mol consumption (Figure 4(a)), the large to small cavity ratio (L/S) was 1.59 and 0.98 for pure water and PVCap systems, respectively. The value of L/S did not follow the theoretical capturing trend ( $L/S = 3$ ) for both systems. This implies that in the initial stage of hydrate formation, small cages were excessively

formed, and in turn the amount of large cages was not sufficient to form perfect unit cells of sl hydrate. A similar observation was reported by Subramanian(1999) et al., who suggested that the formation of the large  $5^{12}6^2$  cavity is the rate-limiting step for hydrate formation. As shown in Figures 4(a) and (b), the L/S value of the PVCap system was less than that of pure water system. This indicates that the PVCap inhibits large cage encapsulation more, thus the Raman band at  $2905\text{ cm}^{-1}$  (corresponding to the large cavities,  $5^{12}6^2$ ) shows smaller intensity. As gas hydrate formation proceeded (shown in Figures 4(c) and (d)), the L/S discrepancy away from the theoretical value was reduced, and ultimately the L/S values approached the theoretical trend.

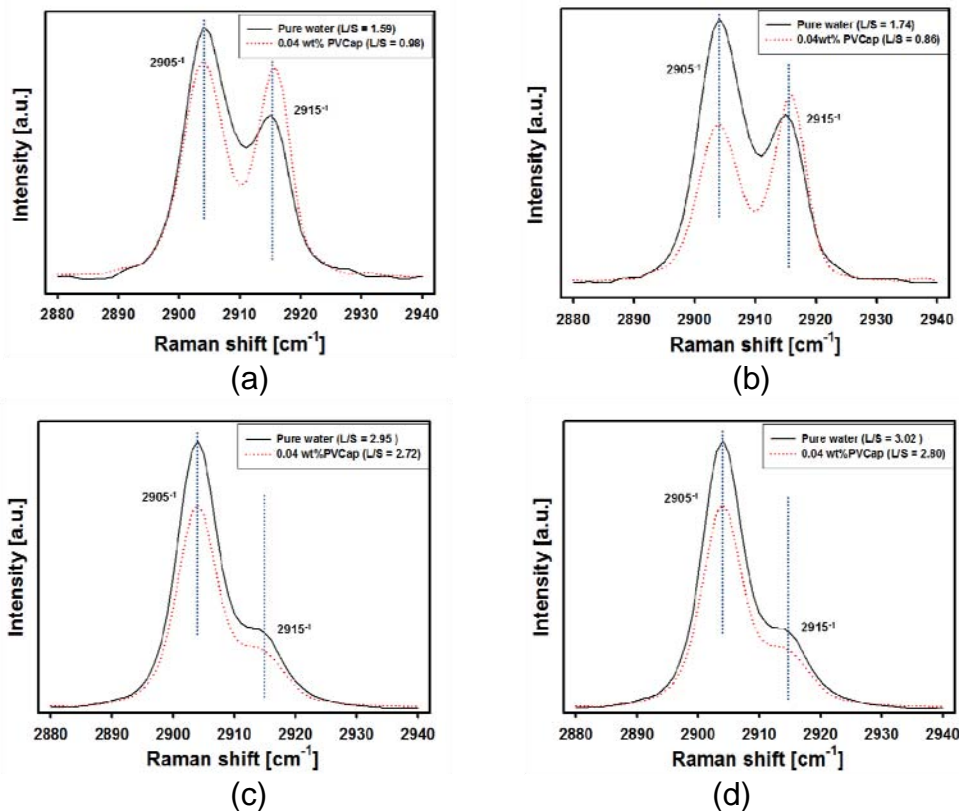


Fig. 4 Raman spectra for  $\text{CH}_4$  hydrate at the same gas consumption; (a)0.08, (b)0.1, and (c)0.3, (d)0.6mol

As many studies (by molecular simulation) have elucidated the adsorption of inhibitors on the surface of gas hydrates, it is believed from our experimental results that PVCap has more strong interactions with large cavities on the sl hydrate surface. These interactions effectively inhibited the large cavity formation and prevented further gas molecular encapsulation (shown in Figure 5)[Kvamme(2005), Koh(2006), King(2000)]. Based on our experimental results, it was also concluded that the inhibition effect of PVCap more successfully acts at an early stage of hydrate formation. As further hydrate formation progressed, the inhibiting effect was gradually reduced, and the cavity ratio also reached the theoretical trend, which was possibly related to the reduced PVCap concentration, by adsorbing on hydrate crystals as a function of time. These results appear to be closely related to the interaction between the lactam ring of PVCap and the

large cavities as many molecular-level studies suggested. Therefore, further studies are required to elucidate this unique behavior.

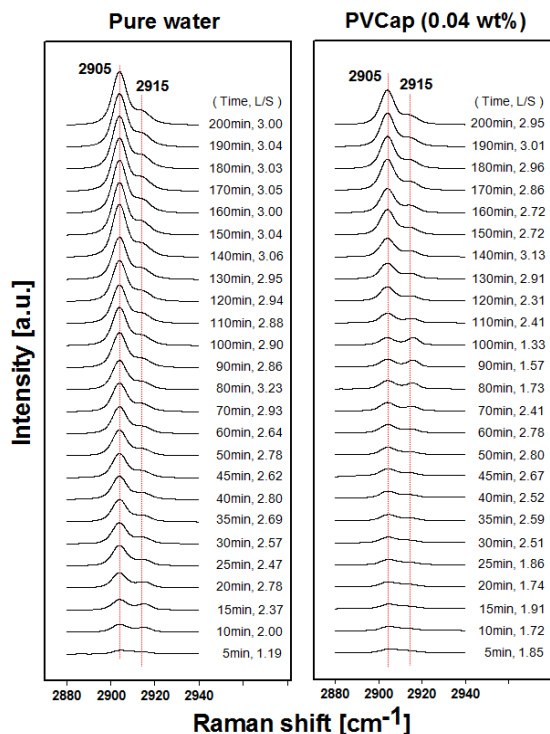


Fig. 5 Comparison of Raman spectra between pure water and PVCap system

### 3. CONCLUSIONS

In this study, we presented an experimental technique in order to collect microscopic (molecular-scale) and macroscopic information on the hydrate formation process. As described in the experimental section, the kinetics of CH<sub>4</sub> hydrate formation and in-situ Raman analysis were simultaneously carried out in a semi-batch stirred tank reactor at constant temperature and pressure. From the result of hydrate kinetics, the presence of PVCap in the system significantly delayed hydrate nucleation and also prevented further gas hydrate formation. During the hydrate formation experiment, in-situ Raman analysis provided time-dependent capturing behavior of guest molecules. In the case of the pure water system, large cavities ( $5^{12}6^2$ ) and small cavities ( $5^{12}$ ) gradually developed with time and approached the theoretical ratio of large to small cavities within several ten minutes. Meanwhile, the system with PVCap showed unstable behavior, and the L/S (large to small cavity ratio) values were also biased from the theoretical cavity ratio. The L/S discrepancy between the experimental and the theoretical values continued until 120 min. It was clearly observed that the Raman intensity of the PVCap system at 2905 cm<sup>-1</sup> corresponding to the large cavities was very much weaker than that of the pure water system for a certain period of time. This observation indicates that the presence of PVCap in the system affects the rate of large cavity encapsulation at an early stage of hydrate formation. As further hydrate formation progressed, the inhibiting effect was gradually reduced, and the cavity ratio

also reached the theoretical trend. The present data and methodologies on the microscopic and macroscopic observations may contribute to better understanding of inhibition mechanisms, and practical applications for flow assurance in gas and oil pipelines.

## REFERENCES

- Kashchiev, D., Firoozabadi, A. (2003), "Induction time in crystallization of gas hydrates", *J Cryst Growth.*, **250**(3-4), 499.
- Kelland, M.A., Svartas, TM., Ovsthus, J., Tomita, T., Chosa, J. (2006), "Studies on some zwitterionic surfactant gas hydrate antiagglomerants", *Chem Eng Sci.*, **61**, 4048.
- Zhang, C.S., Fan, S.S., Liang, D.Q., Guo, K.H. (2004), "Effect of additives on formation of natural gas hydrate", *Fuel.*, **83**, 2115.
- Koh, C.A. (2002), "Towards a fundamental understanding of natural gas hydrates", *Chem Soc. Rev.*, 157-167.
- Sloan, E.D. (1998), "Gas hydrates: Review of physical/chemical properties", *Energy & Fuels.*, **12**(2), 191-196
- Mohammad Reza Talaghah. (2010), "Intensification of the performance of kinetic inhibitors in the presence of polyethylene oxide and polypropylene oxide for simple gas hydrate formation in a flow mini-loop apparatus", *Chem Eng Sci.*, **289**, 129-134
- Sloan, E.D. (2003), "Clathrate hydrate measurements: microscopic, mesoscopic, and macroscopic", *Journal of Chemical Thermodynamics*, **35**(1), 41-53.
- Ehsan Heidaryan., Amir Salarabadi., Jamshid Moghadasi., Alireza Dourbashi. (2010), "A new high performance gas hydrate inhibitor", *Natural Gas Chemistry*, 323-326
- Dalton York, J., Abbas Firoozabadi. (2008), "Comparing effectiveness of rhamnolipid biosurfactant with a quaternary ammonium salt surfactant for hydrate anti-agglomeration", *J. Phys. Chem.*, **11**, 845-851
- Jinhai Yang., Bahman Tohidi. (2011), "Characterization of inhibition mechanisms of kinetic hydrate inhibitors using ultrasonic test technique", *Chem Eng Sci.*, 278-283
- Kelland, M.A. (2006), "History of the development of low dosage hydrate inhibitors", *Energy & Fuels.*, **20**, 825-847
- Makogon, T., Sloan, E.D. (2002), "Mechanism of kinetic hydrate inhibitors", In: *Proceedings of the 4<sup>th</sup> International Conference of Gas Hydrate Yokohama Japan.*, 498-503
- Carver, Drew. and Rodger. (1995), "Inhibition of crystal growth in methane hydrate", *J. Chem. Soc.*, 3449-3460
- Subramanian, S., Slon, E.D.Jr. (1999) "Molecular measurements of methane hydrate formation", *Fluid Phase Equilibria*, 813-820
- Kvamme, B., Kuznetsova, T., Aasolden, K. (2005), "Molecular simulations as a tool for selection of kinetic hydrate inhibitors", *Molecular Simulation*, **31**, 1083-1094
- Koh, C.A., Savidge, J.L., Tang, C.C. (2006), "Time-resolved *in-situ* experiments on the crystallization of natural-gas hydrates", *J. Phys. Chem.*, **100**, 6412-6414
- King, H.E., Hutter, J.L., Lin, M.Y., Sun, T. (2000), "Polymer conformations of gas-hydrate kinetic inhibitors.: A small-angle neutron scattering study", *J. Chem. Phys.*, **112**, 2523-2532